

# Structural and electrical properties of ultrathin niobium nitride films grown by atomic layer deposition

S. Linzen,<sup>1</sup> M. Ziegler,<sup>1</sup> O. V. Astafiev,<sup>2,3,4,5</sup> M. Schmelz,<sup>1</sup> U. Hübner,<sup>1</sup> M. Diegel,<sup>1</sup> E. Il'ichev,<sup>1</sup> and H.-G. Meyer<sup>1</sup>

<sup>1</sup>Leibniz Institute of Photonic Technology, P.O. Box 100239, D-07702 Jena, Germany

<sup>2</sup>Physics Department, Royal Holloway, University of London, Egham, Surrey TW20 0EX, United Kingdom

<sup>3</sup>National Physical Laboratory, Teddington, TW11 0LW, United Kingdom

<sup>4</sup>Moscow Institute of Physics and Technology, Dolgoprudny, 141700, Russia

<sup>5</sup>Russian Quantum Center, 100 Novaya Street, Skolkovo, Moscow region 143025, Russia.

(Dated: September 28, 2016)

We studied and optimised the properties of ultrathin superconducting niobium nitride films fabricated with a plasma-enhanced atomic layer deposition process. By adjusting process parameters, the chemical embedding of undesired oxygen into the films were minimised and a polycrystalline film structure consisting of niobium nitride and niobium grains were formed. For this composition a critical temperature of 13.7 K and critical current densities of  $7 \times 10^6$  A/cm<sup>2</sup> at 4.2 K were measured on 40 nm thick films. A fundamental correlation between these superconducting properties and the crystal lattice size of the cubic  $\epsilon$ -niobium-nitride grains were found. Moreover, the film thickness variation between 40 and 2 nm exhibits a pronounced change of the electrical conductivity at room temperature and reveals a superconductor-insulator-transition in the vicinity of 3 nm film thickness at low temperatures. The thicker films with resistances up to 5 k $\Omega$  per square in the normal state turn to the superconducting one at low temperatures. The perfect thickness control and film homogeneity of the ALD growth make such films extremely promising candidates for developing novel devices on the coherent quantum phase slip effect.

## INTRODUCTION

Nowadays, niobium nitride (NbN) thin films are the best choice for fabricating efficient superconducting single-photon detectors for the visible and near infrared spectrum [1]. Since these detectors have an excellent time resolution and a high signal-to-noise ratio, their application ranges from low photon flux astronomy to quantum cryptography and quantum information processing [2–4]. On the other hand, it was recently argued that the charge-phase duality well known for Josephson junctions (see [5] and references therein) should be observable in circuits with nanowires of highly disordered superconductors in which quantum phase slips can have a significant probability amplitude [6]. Very recently quantum phase slips were observed directly in strongly disordered InO<sub>x</sub>, NbN and TiN nanowires embedded into superconducting loops [7–9].

The most interesting for practical realisation of quantum phase slips as well as for highly efficient photon detectors are the films with thicknesses close to the superconductor-insulator transition [7–10]. Usually, NbN films are deposited by magnetron sputtering [11, 12]. However, it is a challenge to achieve the perfect thickness control for such thin films, since the sputtering rate is rather high. This problem can be solved by making use of atomic layer deposition (ALD) technique where almost perfect thickness control and homogeneity can be obtained. In this work, we report on an optimal set of parameters for fabrication of NbN thin films obtained by a metal organic plasma-enhanced atomic layer deposition (PEALD) process. For these films a correlation between the superconducting properties and the NbN crystal lattice size was observed and a thickness dependent superconductor-insulator transition was demonstrated.

## EXPERIMENTAL

The base of our deposition technique is a standard *OpAL* ALD system by Oxford Instruments Plasma Technology, which has a minimum vacuum chamber pressure of 2 mTorr. This system was upgraded with an inductively coupled remote plasma source (ICP) to realize the plasma-enhanced deposition regime. Further, a nitrogen glove box was added to the open load system of the Oxford *OpAL*. The dry nitrogen atmosphere reduces water contaminations in the ALD reactor during sample handling and processing [13]. The complete ALD setup is installed inside the clean room (ISO class 4) of the Leibniz Institute of Photonic Technology.

As precursor, we used the metal-organic compound (tert-butylimido)-tris (diethylamino)-niobium (TBTDEN). This precursor was produced at our request by the research team of Heraeus Precious Metals, Germany. Further a hydrogen plasma was used in order to optimize the deposition process. The whole PEALD process consisted of numerous deposition cycles repeating always the same four basic steps. First, the substrate is exposed to TBTDEN. After the exposition, the reaction chamber is purged with dry argon and nitrogen. Within the third step, the hydrogen radicals provided by the remote ICP reduce the chemically bonded monolayer of TBTDEN and generate NbN. Finally, the reaction chamber is purged again with dry argon and nitrogen. Due to the self-limiting single surface reactions of each precursor, one cycle produces under ideal conditions one monolayer of NbN. Because of the large size of the TBTDEN molecule, however, steric hindrance occurs resulting in a growth rate much smaller than one monolayer per cycle. We obtain experimentally a constant value of 0.046 nm/cycle within a wide film thickness range of 3 to 80 nm. Thus, the desired film thickness can be precisely

controlled and adjusted by the number of cycles.

Due to the occurrence of a variety of crystal phases with similar chemical composition [14] but very different electrical properties, the deposition of superconducting NbN thin films is non-trivial. Our first ALD films with a thickness of 40 nm exhibited a relatively low critical temperature  $T_C$  of 10.2 K as well as a critical current density  $J_C$  at 4.2 K of  $9 \times 10^5$  A/cm<sup>2</sup> [13]. However, it is well known that the  $\epsilon$ -NbN phase reaches a bulk  $T_C$  of about 16 K [15]. Thus, motivated by this difference, our investigations were focused firstly on searching for an optimum ALD process parameter set for 40 nm thick films to reach a chemical composition as close as possible to the 1:1 ratio between niobium and nitrogen. We deposited NbN thin films by making use of different process parameters (for instance, plasma pressure, plasma duration, substrate temperature) and the atomic ratio was measured. For this purpose we used the Rutherford backscattering spectroscopy (RBS) with 1.4 MeV  ${}^4\text{He}^+$  ions representing an integral composition within a film volume of about 1 mm<sup>2</sup>  $\times$  40 nm. As a result, we found that the films are always contaminated with oxygen. The best niobium-nitrogen-oxygen atom relation, i.e. the one with nearly the same amount of niobium and nitrogen as well as the lowest oxygen content, is found to be 48:41:11.

The detected undesirable incorporation of oxygen is caused by the higher chemical binding energy of Nb-O in comparison to Nb-N. Thus, the small oxygen or water impurities in the deposition vacuum chamber and in the precursor are sufficient as effective oxygen sources. We do not observe a significant change in the chemical composition by reducing the film thickness from 40 nm down to less than 10 nm. For films with an increased thickness of 80 nm or more, however, additional oxygen enrichment on the film surface and within the film-substrate interface is detectable. Here the very long deposition times of more than one day seem to amplify oxygen interdiffusion processes.

Nevertheless, the ALD films fabricated with an optimum process parameter set exhibit significantly improved superconducting properties (see below) and chemical composition in comparison to our first superconducting films in spite of the fact that a pure 1:1 niobium to nitrogen composition is not achieved yet. By making use of X-ray photoelectron spectroscopy (XPS) one can conclude that beside the aimed niobium nitride there is a complex coexistence with niobium, niobium oxides and niobium oxo-nitrides within the entire thin film. Further, impurities of hydrogen and carbon were detected by secondary ion mass spectroscopy (SIMS) which will be described elsewhere in detail [16].

## RESULTS AND DISCUSSION

The crystalline part of our thin NbN PEALD films could be revealed by X-ray diffraction analysis (XRD). We used a *X'PERT Pro* diffractometer from PANalytical B.V., in which the Bragg-Brentano geometry and cooper  $K_\alpha$  radiation are applied. Figure 1 shows a typical  $\theta - 2\theta$ -scan of a 40 nm thick

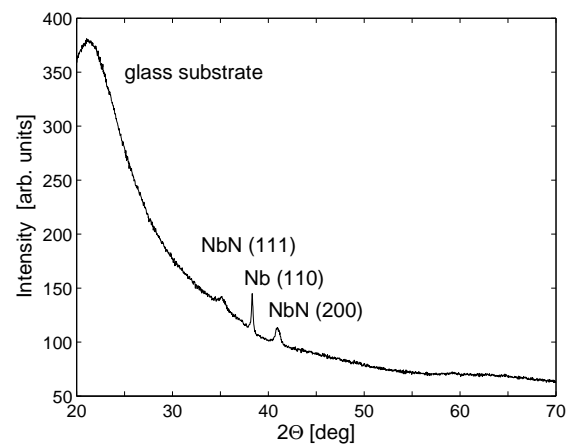


FIG. 1: XRD  $\theta - 2\theta$ -scan of a 40 nm thick NbN film grown on an amorphous quartz glass substrate by PEALD. The experimental data shows reflections from niobium nitride as well as from pure niobium crystalline film parts.

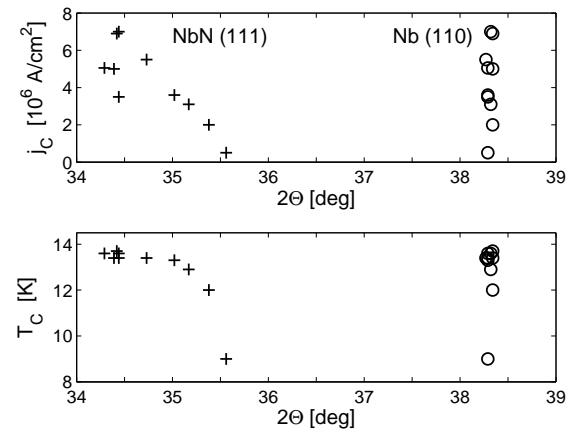


FIG. 2: Superconducting properties  $T_C$  and  $J_C$  of 40 nm thick NbN films as a function of their crystal structure represented by the XRD  $2\theta$  peak positions of NbN(111) and Nb(110). Note the strong correlation of  $T_C$  and  $J_C$  with the NbN(111) peak position, whereas there is no correlation with the Nb(110) reflection i.e. the lattice parameter of the niobium grains.  $T_C$  was defined as the 10 % value of the resistance at 20 K ( $R_{20}$ ).  $J_C$  was determined at 4.2 K with an alternate current of 0.05 Hz and a voltage criterion of 10  $\mu$ V.

film grown with optimum PEALD parameters on a quartz glass substrate. The pattern indicates, onto the broad background of the amorphous glass, three peaks of moderate intensity, which correspond to the Nb and NbN crystal lattices. The Nb (110) reflection at 38.32° is sharp with a full width at half maximum (FWHM) of only 0.17°, whereas the NbN (111) reflection at 35.17° and the NbN (200) reflection at 40.94° are widened with FWHM values of 0.46° and 0.52°, respectively. Thus, the NbN grains exhibit a pronounced lattice parameter spread. This interesting finding can be used for study thin films transport properties as a function of the value of the lat-

tice parameter.

Indeed, using different plasma duration times, we fabricated NbN thin films with parameter  $a$  ranging between 4.369 Å and 4.526 Å. These values are reconstructed from the (111)-peak position of the  $2\theta$  scan, which is similar to presented in Fig. 1.  $T_C$  and  $J_C$  as a function of the parameter  $a$  (representing by the NbN (111)-peak position) are shown in Fig. 2. From this figure, an increase of the critical temperature of our ALD-deposited films is clearly to be seen with increasing the lattice parameter  $a$  of the cubic  $\epsilon$ -NbN unit cell. An origin of this dependence required further study. For comparison let us note that  $a = 4.442$  Å for bulk  $\epsilon$ -NbN [17].

On the other hand, there is no influence of the crystalline niobium film part to the superconducting properties. The lattice parameter is nearly fixed at 3.321 Å or the (110) peak position at 38.30° (see Fig. 2). The details of the coexistence of the NbN and Nb lattices within the prepared ALD films are required further study. Nevertheless, the reached high  $T_C$  of 13.7 K and  $J_C$  of  $7 \times 10^6$  A/cm<sup>2</sup> at 4.2 K as well as their dependencies on the lattice parameter  $a$  of NbN agrees with a structural model, in which the distances between the NbN crystallites are smaller than the coherence length.

We reproduced the detected correlation between the superconducting properties and the crystal lattice size of the NbN grains by variation of further deposition parameters, too. Thus, this correlation has a fundamental character. For the further investigations we fixed the optimum parameters plasma duration time at XXX s, the substrate temperature a XXX C and the plasma pressure at XXX Pa.

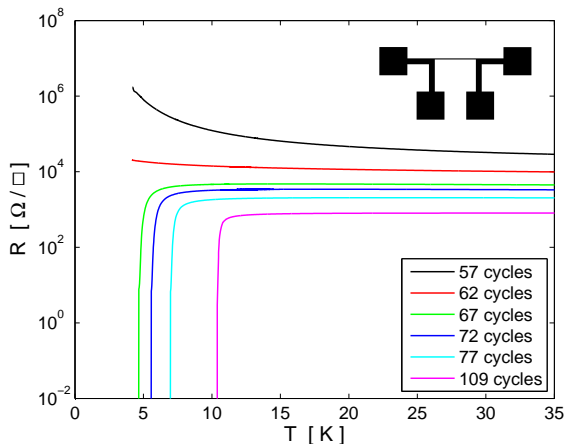


FIG. 3: The temperature dependence of the square resistivity  $R(T)$  for samples with different thickness between 2.6 and 5.0 nm. One ALD cycle corresponds to 0.046 nm of the film thickness.  
Inset: Layout of the realised film bridge structures for the four point  $R(T)$  and  $J_C$  measurements. The NbN bridge in the middle between the contact pads has a length of 300 μm and a width of 5 μm. The  $R(T)$  curves were obtained with a temperature resolution of better than 0.1 K.

By making use of the optimized deposition process, we investigated the influence of a films thickness on their transport properties. The film thickness was varied from 40 to 2.6 nm

by reducing the number of ALD plasma cycles from 870 to 57. For electrical measurements well-defined bridge structures (see inset of Fig. 3) were chemically etched into the NbN films and bonded on a carrier system. The bridge lengths were 300 μm with the widths of 5 μm. We observe an only small influence of the film thickness on the electrical properties down to a thickness of about 10 nm. For the latter,  $T_C$  is reduced by 1.7 K and the room temperature resistance is increased by about 30 % in comparison to the values for 40 nm thick films ( $T_C = 13.7$  K,  $\rho = 2.5$  μΩ × m). However for films thinner than 10 nm, the film thickness plays an important role (see Fig. 3). At 3.1 nm NbN film thickness (corresponding to 67 plasma cycles) we still observe a superconducting transition with a  $T_C$  of 4.6 K. For that film, the normal state resistance reaches 5 kΩ/□, which is very promising for applications using coherent quantum phase slips. The high resistance is then directly translated into high kinetic inductance and shallow tunnelling barrier for fluxes in nano-wires [7]. Note also that there is no signature of the non-zero resistance down to less than  $10^{-2}\Omega$  per square – six orders of magnitude lower than the normal state resistance. Films with a thickness smaller than 2.9 nm show no superconducting but insulating behavior at low temperatures, as it can be seen in Fig. 3. Thus, a thickness dependent superconductor-insulator transition for the ALD thin NbN films is experimentally observed, and first experiments with structures employing coherent quantum phase slips are in progress.

## CONCLUSION

We have optimised our PEALD process for the growth of ultrathin superconducting NbN films. A critical temperature of 13.7 K were reached for 40 nm film thickness. The realised polycrystalline film structure of niobium nitride and pure niobium grains could reproducibly be fabricated down to a thickness of 2 nm. The films exhibit a well pronounced superconductor-insulator-transition depending on their thicknesses and don't show any signatures of normal resistance, when they turn to the superconducting state at low temperatures.

The pronounced superconductor-insulator-transition, the high resistances of the superconducting films in the normal state together with the accurate thickness control make the films excellent candidates for new generation of cryo-electronic devices with nano-wires and constrictions utilising quantum phase slips. The devices are of particular interest for the realisation of current standards dual to the common voltage standards on the basis of conventional Josephson junctions.

## ACKNOWLEDGEMENT

We would like to thank Ch. Schmidt for XRD measurements as well as L. Fritsch and S. Goerke for support with

the ALD technique.

OVA acknowledges a hospitality of the IPHT and a partial support of Royal Society within International Exchanges Scheme (2015 Russia RFBR #15-52-10044 KO a Cost share), and Russian Scientific Fund (N 15- 12-30030).

A. A. Korneev, I. M. Charaev, A. V. Semenov, G. N. Goltsman, L. B. Ioffe, T. M. Klapwijk, and J. S. Tsai Phys. Rev. B **88**, 220506(R) (2013).

- [9] J. T. Peltonen, Z. H. Peng, Yu. P. Korneeva, B. M. Voronov, A. A. Korneev, A. V. Semenov, G. N. Goltsman, J. S. Tsai, O. V. Astafiev, arxiv:1601.07899 (2016).
- [10] M. Hofherr, D. Rall, K. Ilin, M. Siegel, A. Semenov, H.-W. Hbers, and N. A. Gippius, J. Appl. Phys. **108**, 014507 (2010).
- [11] E. J. Cukauskas , W. L. Carter and S. B. Qadri, J. Appl. Phys. **57**, 2538 (1985).
- [12] J. J. Olaya, S. E. Rodil and S. Muhl, Thin Solid Films **516**, 8319 (2008).
- [13] M. Ziegler, L. Fritzsch, J. Day, S. Linzen, S. Anders, J. Toussaint and H.-G. Meyer, Supercond. Sci. Technol. **26**, 25008 (2013).
- [14] G. Brauer und R. Esselborn, Nitridphasen des Niobs, Z. anorg. allg. Chemie **309** 151 (1961).
- [15] G. Horn und E. Saur, Prparation und Supraleitungseigenschaften von Niobnitrid sowie Niobnitrid mit Titan-, Zirkon- und Tantalzusatz, Z. Phys. **210**, 70-79 (1968).
- [16] M. Ziegler, S. Linzen et al., in preparation.
- [17] R.E. Teece, M.S. Osofsky, E.F. Skelton, S.B. Qardi, J.S. Horwitz, D.B. Chrisey, Phys. Rev. B **51**, 9356 (1995).

- 
- [1] A. Semenov, G. Goltsman, and A.Korneev, Quantum detection by current carrying superconducting film, Physica C **351**, 349, (2001).
  - [2] Robert H. Hadfield, Nature photonics **3**, 696 (2009).
  - [3] N. Gisin, G. G. Ribordy, W. Tittel, and H. Zbinden, Rev. Mod. Phys. **74**, 145 (2002).
  - [4] M. Halder, A. Beveratos, N. Gisin, V. Scarani, C. Simon, and H. Zbinden, Nature Physics **3**, 692 (2007).
  - [5] G. Schön and A.D. Zaikin, Phys. Rep. **198**, 237 (1990).
  - [6] J. E. Mooij and Yu. V. Nazarov, Nature Physics **2**, 169 (2006).
  - [7] O. V. Astafiev, L. B. Ioffe, S. Kafanov, Yu. A. Pashkin, K. Yu. Arutyunov, D. Shahar, O. Cohen, J. S. Tsai, Nature **484**, 355 (2012)
  - [8] J. T. Peltonen, O. V. Astafiev, Yu. P. Korneeva, B. M. Voronov,